Technical Considerations for ACHD Imaging

Andrew M. Crean

Contents

1 Introduction

There are now more adults alive with congenital heart disease than children (Marelli et al. 2007), and many will have ongoing problems despite surgical repair. Surgery is never a cure—merely a fix—and in some cases directly introduces new problems that were not present previously (Celermajer and Greaves 2002). ACHD patients therefore generally require lifelong follow-up in specialized institutions where the technical and clinical expertise exists to recognize and deal with issues as they arise.

Imaging lies at the heart of this follow-up process. Today we have so many advanced modalities to choose from that a nonimager may be bewildered by the options available and uncertain about what test would best answer the clinical problem facing him or her. The purpose of this chapter is to review briefly the strengths and weaknesses of the major cardiac imaging modalities and propose a few principles to help guide the selection of most appropriate modality in each case. It should be recognized that this is a single author opinion, and—as with everything else in medicine—there is more than one way to skin a cat! Nevertheless the principles here are expected to be non-contentious and largely self-evident.

A.M. Crean, M.R.C.P., F.R.C.R.
Sanghvi Endowed Chair in Cardiovascular Imaging
Professor of Cardiology and Pediatrics, University of Cincinnati Medical Center and Cincinnati Children's Hospital Medical Center,
Cincinnati, OH, USA
e-mail: andrewcrean@gmail.com

Med Radiol Diagn Imaging (2018)
DOI 10.1007/174_2017_169, © Springer International Publishing AG
Published Online: 05 April 2018

2 What Information Do We Want?

In imaging the key question to the referrer should always be: 'what do you want to know?'. An uncertain or unfocussed question is unlikely to result in a lucid and helpful report. Lack of clarity in the request may also lead to incorrect selection of modality. Clear communication between the referrer and the imager is therefore vital for appropriate triage and protocolling of requests. The imager cannot however entirely rely on the referrer to provide all essential knowledge, and it is incumbent upon an ACHD imager to review prior imaging and—on occasion—the hospital notes as the underlying anatomy and physiology (and even the patient's personality) may dictate the most appropriate imaging technique to use.

In general terms, however, the commonest type of information required in ACHD patients pertains to anatomy, function and flow. These and other potential requirements are summarized in Table 1.

Table 1 Areas of potential interest in an ACHD imaging examination

Anatomy
Cardiac anatomy
Bronchial anatomy
Visceral situs
Anomalies of systemic and/or pulmonary venous return
Anomalies of the aorta and/or branch vessels
Physiology
Ventricular volumes
Ventricular function
Flow
Peak velocity across stenoses
Volume of forward and regurgitant flow
Direction of flow
Quantification of shunts
Perfusion
Reimplanted coronary arteries
Compressed or stenosed coronary arteries
Aneurysmal coronary arteries
Assessment of functional reserve prior to major surgery
Tissue characterization
Ischaemic scar
Myocardial oedema
Subclinical fibrosis
Calcium
Metal
Thrombus
Within cardiac chambers
Within aneurysmal coronary arteries
Within pulmonary arteries
Postsurgical complications
Anatomic distortion
Infection
Leakage
Resolving conflicting information

3 Imaging Anatomy

Understanding the anatomy of the patient is fundamental to ACHD care. Many conditions have seen era-based variations in surgical repair, leading to very different anatomic appearances—for example, a *d*-TGA patient repaired 40 years ago by a Mustard or Senning procedure has quite different anatomy to the same patient repaired by the arterial switch operation which is the standard of care today (Roche et al. 2011).

Basic anatomy can be inferred to some degree from the plain CXR with PA and lateral views. Heart size and bronchial situs, great vessel anatomy and pulmonary arterial and venous anomalies may all be recognized by plain film. Inferences about physiology may even be made based on atrial chamber enlargement, pulmonary venous distension and lung parenchymal lymphatic engorgement. However it is hard to argue that a two-dimensional representation of the chest represents the standard of reference in first-world countries any longer. One useful feature of the CXR remains its ability to depict small stainless steel devices, clips or coils that may have been used in childhood to close holes or embolize vessels. Many of these devices cause substantial disturbance to the uniformity of a magnetic field and result in large signal voids on CMR images (Fig. 1). Recognition of these in advance is useful so that limited magnet time is not wasted.

Although echocardiography is usually the first imaging test experienced by the ACHD patient, it is in fact probably the least well suited to questions of pure anatomy. Image quality is both operator and patient dependent. Obesity, in particular, challenges the echocardiographer in a way that is rarely

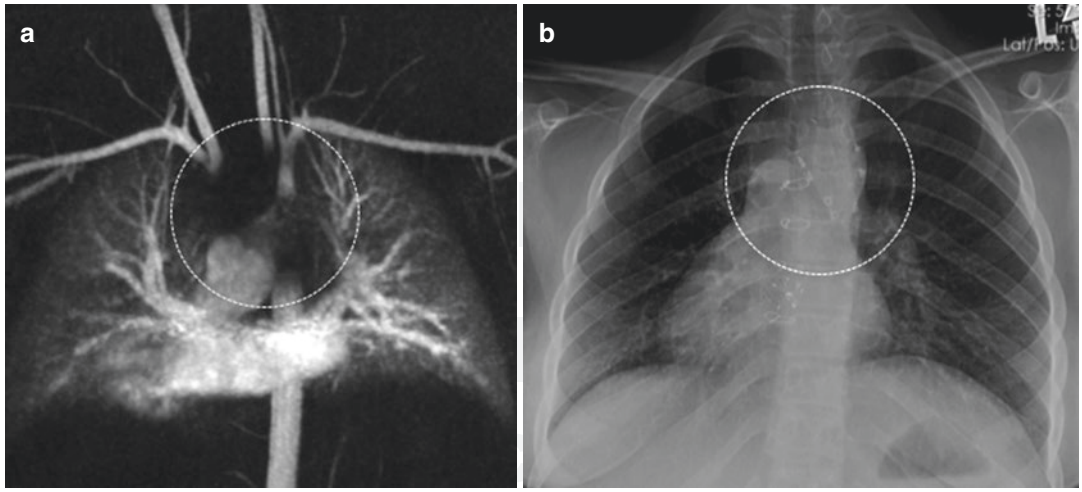

Fig. 1 Artefact due to stainless steel coils. (**a**) MR angiogram in a patient with a Fontan circuit shows a large central area (dotted circle) where the underlying anatomy is obscured. (**b**) CXR in same patient (note incidental dextrocardia) reveals multiple metallic densities in the central mediastinum (dotted circle) from venous embolization with stainless steel coils

a problem for CT or CMR (assuming the patient does not exceed the maximum table weight and can physically fit into the scanner). Although image acquisition is usually standardized, this is in the form of selective 2D tomographic views selected by the operator at the time of the scan. There is no possibility to return to the data and reconstruct further views desired after the fact. This limitation of standard 2D echo has only partially been overcome by 3D techniques (Yang 2017). These remain cumbersome, imperfect (Crean et al. 2011) and far from routine in the majority of laboratories. The other major limitation of echo pertains to its inability to visualize more than the proximal portions of the vascular structures of the thorax or to interrogate the lung parenchyma beyond basic recognition of pleural fluid and lung collapse/consolidation. Therefore, although echocardiographic assessment is vital in ACHD for other reasons, assessment of anatomy alone is rarely its forte.

What then should we use to determine the thoracic anatomy of the ACHD patient with confidence? If anatomy is the sole or primary question, there is little doubt that computed tomography (CT) is the test of choice in many patients (Han et al. 2015a). Advances in technology have been so profound that imaging of the chest by CT now takes only a few seconds. Images can be acquired in most ACHD patients at trivial doses of radiation. Low-dose imaging is possible for two reasons. Firstly, many complex ACHD patients are well below mean adult size due to chronic illness, and a relative lack of obesity means that images contain less noise. Secondly—as a corollary to the first point—low body mass index means that tube voltage may usually be reduced down to 80 kV rather than the standard 120 kV resulting in an exponential decrease in radiation exposure (Han et al. 2015b). The additional noise created by this approach is usually tolerable for all but the smallest structures and can be smoothed out by both iterative reconstruction techniques or simply by reconstructing at thicker slice thickness than that acquired (Fig. 2).

There are additional benefits of anatomic imaging by CT. Many of the peculiarities of ACHD can be relatively subtle—small communications between structures, anomalous vessels including aorta-pulmonary and veno-venous collaterals, pulmonary arteriovenous malformations, etc. may all be missed without high spatial resolution. This is an inherent advantage of CT where it is possible to acquire volumes of isotropic data with a voxel size of 0.5 mm^3 at still acceptable radiation exposure levels. Such high-resolution data sets have the further advantage of potential reconstruction in any non-standard imaging plane required to best demonstrate the abnormality, long after the patient has departed the CT suite. The ability to synchronize

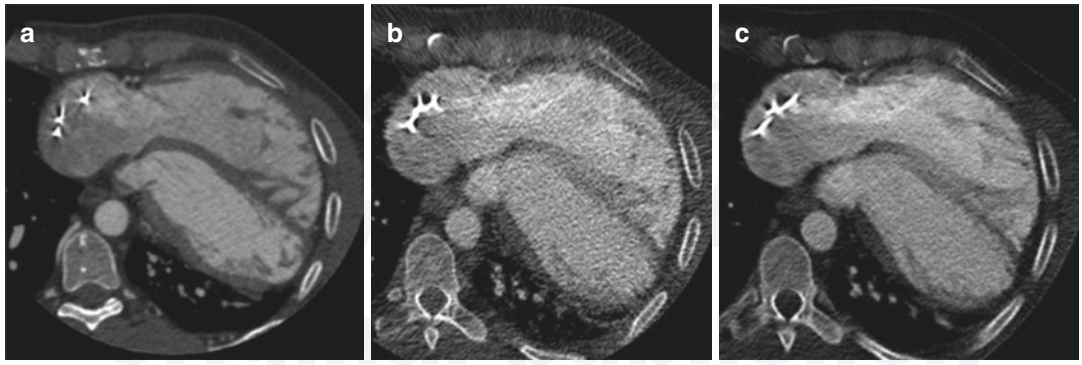

Fig. 2 Decreasing dose in cardiac CT through kV manipulation. (**a**) Axial cross section by CT in 2008 in a patient with tetralogy of Fallot acquired at 0.5 mm, **120 kV**, multiphase. Image quality is excellent with little noise but the total effective dose was 25 mSv. (**b**) Same patient re-imaged in 2010 at 0.5 mm, **80 kV**, multiphase. The image is significantly noisier but still interpretable. (**c**) Same data set as in (**b**) but this time the slice *has been thickened post acquisition to 5 mm rather than the native 0.5 mm*. Note how much of the image noise is reduced by this manoeuvre with little change in diagnostic quality for the major cardiac structures

CT image acquisition to the ECG also makes it particularly suitable for anatomical assessment of the aortic root and coronary arteries which are otherwise obscured by cardiac motion. The principal disadvantage of anatomic imaging by CT is the need for administration of intravenous contrast. This slows the workflow and may be contraindicated in patients with reduced renal function or severe contrast allergy.

CMR anatomic imaging is usually performed as part of any cardiac study. Sequences may use bright blood techniques in which the blood pool is seen as higher signal intensity than surrounding myocardium or black blood techniques in which the signal from flowing blood is suppressed. Compared to CT, anatomic CMR imaging incurs a considerable time penalty (10–15 min for bright blood imaging of the thorax by CMR versus under 5 s by CT) and is obtained at significantly lower spatial resolution. Despite this, many centres employ CMR as the primary tool for assessment of the ACHD patient. This is not because it is a better anatomic test than CT but because other information (particularly ventricular size and function) is usually also desired.

However there are rare situations when CMR may be used principally for anatomy. The most common indication for this at our centre usually involves a pregnant woman with a known aortopathy (Marfan syndrome, coarctation patch aneurysm) who develops chest pain—rapidly leading to similar symptoms in the responsible clinician! Although CT may be the most logical test for patients in the second trimester or beyond, the spectre of unproven 'risk' to the foetus almost invariably results in both patient and physician insisting upon CMR. This may not be a trivial undertaking in a heavily pregnant woman who may need to lie partially elevated to prevent IVC compression and who is usually uncomfortable and restless. Limited diaphragmatic excursion results in poor breath holding and frequently suboptimal images. Furthermore, gadolinium is relatively contraindicated in pregnancy (Garcia-Bournissen et al. 2006; Sundgren and Leander 2011). Here, however, one advantage of CMR over CT emerges. Steady-state free precession (SSFP) pulse sequences generate intrinsic contrast within the blood pool without the need to inject exogenous agents (Fig. 3). Furthermore, the use of free-breathing navigated SSFP sequences can obviate concerns about poor breath holding (Stehning et al. 2005).

Cardiac catheterization should not be forgotten as a method for determining anatomy. Indeed in the early days of congenital heart disease, it was the principal if not the only way to assess complex intracardiac anatomy. Whilst that role has largely been usurped by echo and other cross-sectional techniques, it remains useful for assessment of vascular structures particularly where intervention is contemplated (e.g. delivery of coarctation or pulmonary artery stent, collateral embolization). The direct injection into collateral

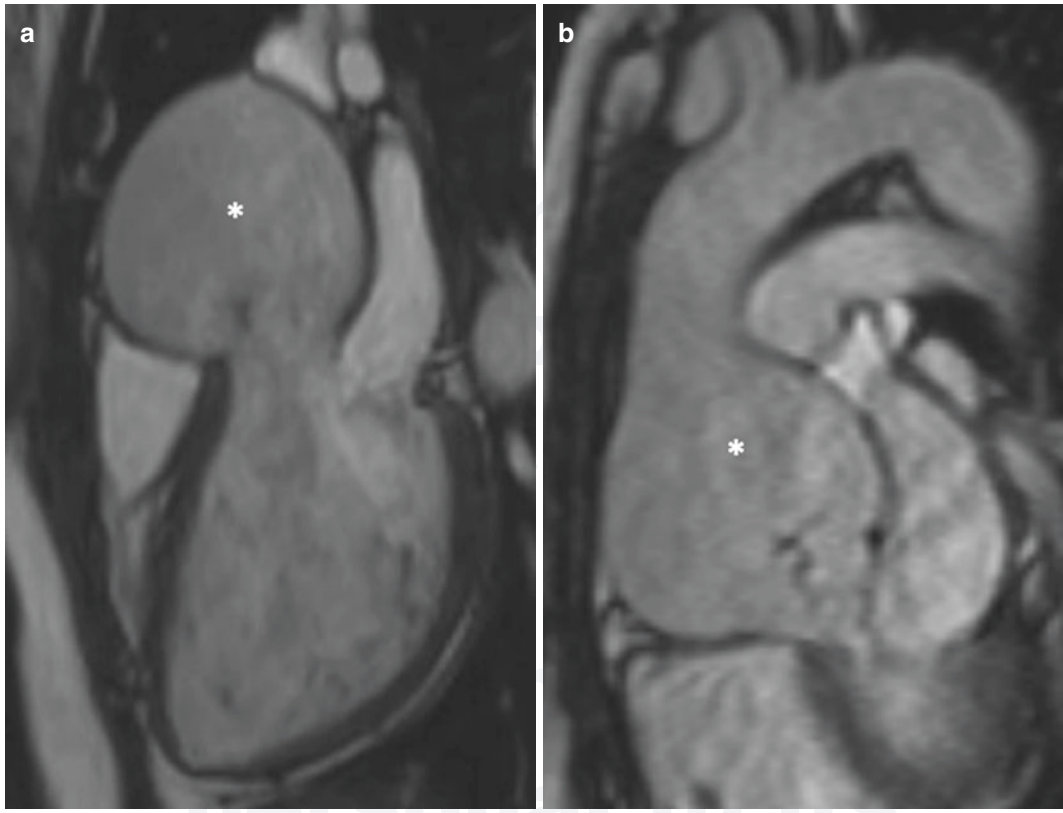

Fig. 3 Examples of severe aortic root dilatation in two different pregnant patients with Marfan syndrome. To avoid administering gadolinium—and limit heating of the foetus by radiofrequency deposition—single-shot steady-state free precession imaging has been used. In both cases the aortic root (asterisk) measured almost 6 cm across (normal is less than 4 cm; 5 cm is the usual operative threshold in Marfan syndrome)

vessels may also reveal the course and extent of these more clearly than simply relying upon passive filling by contrast as happens at CT or CMR.

We close this section with nuclear medicine, only to comment that the limited spatial resolution of this technique results in little or no role for anatomical imaging of the ACHD patient. It may still have some limited role in physiologic imaging which will be discussed subsequent sections.

	Echo	Nuclear	CT	CMR	Cath
Spatial resolution	++	+	++++	++	++++
Temporal resolution	++++	+	++	+++	++++
Suitability in obese	++	+	++++	++++	+++
Multiplanar reformats possible	–	++	++++	+++	–
3D reconstructions possible	–	++	++++	+++	–
Limited by metal	++	+++	+	+++	–
Limited by calcium	+	+	+	++	–
Speed of assessment	++	++	++++	+	+++
Requires exogenous contrast injection	–	++++	+++	+	++++
Availability	++++	++++	++++	++	++++
Claustrophobia	–	+	++	+++	–
Radiation	–	+++	+/++	–	++/+++

4 Imaging Ventricular Function

One of the most frequently asked questions of an ACHD imager pertains to the size and function of the ventricles. Accurate assessment is vital since serial follow-up is often performed in order to determine the most appropriate time to intervene on lesions which are responsible for ventricular enlargement or impairment of ventricular function. Although 2D echo is most frequently used for this purpose, its accuracy and interobserver variability leave much to be desired. Endocardial definition is often poor, and, since a volume of data is not acquired, size and function are estimated in ways that make assumptions about the shape of the ventricles. Such assumptions are frequently untrue in normal hearts and are quite unreliable in malformed or repaired hearts. 3D echo has been shown to be more accurate and precise in the paediatric population, but the size of enlarged ventricles (particularly the RV) in adults often results in incomplete coverage of the ventricle within the sector field of view and can lead to quite significant underestimation of ventricular volume (Crean et al. 2011).

CMR is generally regarded as the standard of reference for functional and volumetric assessment of the ventricles, notwithstanding occasional dissenters (DeFaria Yeh and Foster 2014; Geva 2014). Sequential slices are acquired in a 2D fashion, and then the resulting stack of discs is contoured offline and provides measurements derived from Simpson's rule. Since the precise geometry of the ventricle is accounted for in the image acquisition, there are no geometric assumptions made. Values derived in this way are usually highly reproducible both within and between observers (Mooij et al. 2008; Moody et al. 2015). Nonetheless there are several technical considerations of which to be aware. CMR cine images, as conventionally acquired, do not in fact reflect real-time motion data—in other words the image as seen is not constructed from motion data pertaining to a single cardiac cycle. Instead, using a process of 'segmented acquisition', the cine data required to build a moving cine image at any one slice location is acquired over multiple temporally sequential cardiac cycles. In practice this means that each moving image is usually the result of a data acquisition process over 10–15 heartbeats. There are several implications of this: (a) the temporal resolution (i.e. frame rate) of each cine image is a function of how many heartbeats are used to acquire data, better temporal resolution can be achieved by collecting more data over more heartbeats but at a cost of a longer breath hold; (b) since the image data is derived from sequential beats, stable sinus rhythm is a prerequisite for clear images free of the temporal blurring which can make contouring unreliable. Although there are methods for acquiring a cine slice in a single heartbeat ('single-shot imaging'), the resulting image is often low in both spatial and temporal resolution, and since each slice is acquired from beats of different cycle length, the varying number of cardiac phases per cycle means that conventional contouring packages (which require each slice to have the same number of phases) cannot load the data for quantitative measurement. Finally, published normal ranges exist with different values—how is this possible? The answer for the LV depends on whether the papillary muscles are ignored ('left in the blood pool') or included when drawing the endocardial contour (Alfakih et al. 2003a; Buechel et al. 2009; Hudsmith et al. 2005; Cain et al. 2009; Salton et al. 2002; Lorenz et al. 1999; Sievers et al. 2004). Novel planes of acquisition may also affect the ideal normal range (Childs et al. 2011; Clay et al. 2006).Values may differ for the RV according to whether the ventricle was contoured from the axial, short axis or some other plane (Maceira et al. 2006; Alfakih et al. 2003b; James et al. 2013; Fratz et al. 2009; Strugnell et al. 2005; Winter et al. 2008). It is therefore important that each CMR lab maintain a consistent approach to contouring and use of the appropriate normal range. Very recently, work produced from the UK Biobank project has provided normal sex and age-defined ranges in over 5000 healthy individuals, and this is likely to become the standard reference paper in this area—at least for Caucasian populations (Petersen et al. 2017).

Cardiac CT is being utilized at most ACHD centres with volumetric and functional assessment an increasingly common indication. Usually

this is requested in patients who are either claustrophobic or have implanted devices and thus contraindicated for CMR. There have been several reports suggesting comparable accuracy to CMR for volumetric assessment (Fuchs et al. 2016; Koch et al. 2004; Juergens et al. 2004; Mahnken et al. 2003; Singh et al. 2014). Caveats relate not only to the nature of the populations studied which were invariably small and free of congenital heart disease but also to the CT equipment employed in the majority of studies frequently involving dual-tube technology resulting in a potential temporal resolution considerably superior to many other types of scanner. It is necessary to understand that the ability to construct a time-volume ventricular filling curve accurately is a function of not only the patient's heart rate but also the effective temporal resolution of the scanner used. This latter itself can vary according to the scan mode selected. As usual in cardiac imaging, there is no substitute for understanding how image acquisition occurs.

Nonetheless, there is no doubt that cardiac CT provides measurements of end diastolic volume that are usually highly reliable. End systolic volume (and therefore ejection fraction) measurement accuracy depends on sufficient temporal resolution. Therefore an apparently impaired ventricle may be either genuinely impaired or apparently so because true end systolic images have not been acquired. Distinction between genuine and artificial ventricular impairment may be difficult unless the other ventricle demonstrates entirely normal function. Since it is difficult to overestimate ejection fraction (EF) by CT, normal function on one side makes it more likely that true end systole has been captured and therefore that the abnormal function on the other side is more likely to be genuine. One final caveat is that since most CT scanners acquire cine data by segmentation, they are as vulnerable to irregular cardiac cycles as CMR.

In cases where CMR is not possible and CT and echo give conflicting results, use of radionuclide angiography should not be forgotten (Schelbert et al. 1975; Harel et al. 2007; Navare et al. 2003; Johnson and Lawson 1996; Hesse et al. 2008). This is a simple and reliable technique for either ventricle. Since images are acquired by averaging over hundreds of heartbeats, the technique is also relatively independent of cycle length variations. Careful attention must be paid to correctly defining the boundary of the ventricle. This may be difficult for technologists unfamiliar with congenital hearts, particularly if there are abnormalities of situs or looping. It is often wise for the ACHD imager to directly inspect the raw data to ensure ventricles have been correctly identified and encircled.

Finally, visual assessment of ventricular function by conventional angiography is still a valid approach even if it appears to lack the rigour of cross-sectional imaging. The temporal resolution of angiography is so high that reliable visual estimates of function can be made even in the presence of arrhythmia in most cases.

5 Imaging Pressure and Flow

Abnormalities of flow are fundamental to many of the conditions seen in congenital heart disease. Reliable methods are required to measure both velocity and volume of flow (Lotz et al. 2002). On occasion it may be useful to additionally have information about direction of flow. The commonest requirement is for flow assessment across a valvular lesion where varying degrees of stenosis and regurgitation may coexist. Not infrequently there may also be questions regarding the flow across conduits—which often calcify and stenose with time—as well as differential flow into branch pulmonary arteries. Aortic flow may be requested in the setting of aortic coarctation. In cases of multiple sources of pulmonary blood flow (i.e. some or all of the blood flow being derived from collateral sources and not simply the pulmonary arteries), then summed flow of all four pulmonary veins may be required in order to calculate total pulmonary resistance according to the equation: **PVR = 80 * (Mean Pulmonary Artery Pressure - Left Atrial Pressure)/ Pulmonary Flow.** Calculation of pulmonary arterial and aortic flows is also required in the setting of shunt lesions where the shunt fraction has to be calculated.

Echo is once again on the front line for these requests but usually only manages to provide partial answers. There are a number of reasons for this including the previously mentioned problems with poor visualization in a proportion of patients. For isolated valvular stenosis in patients with suitable body habitus, echo estimates peak and mean gradients with a high degree of reliability and reproducibility. Regurgitant lesions are typically more difficult to quantify since all available echo methods are surrogates for the true regurgitant volume which echo cannot measure directly. Echo also struggles with conduit stenosis since the Bernoulli assumptions break down often leading echo to overestimate gradients.

CMR is complementary to echo in many cases. Its strengths are the mirror image of echo in that direct measurement of aortic and pulmonary regurgitant fractions is straightforward and reliable (Mercer-Rosa et al. 2012). Atrioventricular regurgitation may also be directly calculated although is not routinely performed. Net forward flow measurements in the main pulmonary artery and aorta permit calculation of the shunt ratio (Q_p:Q_s) in shunt lesions such as atrial septal defect or patent ductus arteriosus. CMR is also the only available method for measuring total pulmonary blood flow in conditions where some of the arterial supply to the lungs is not derived from the pulmonary arteries. In this circumstance, the total blood supply *to* the lungs is equivalent to the total blood volume returning *from* the lungs (Grosse-Wortmann et al. 2007). Thus measurements of blood flow in each of the pulmonary veins may be summated to provide a rough assessment of total pulmonary flow, which is required for the calculation of pulmonary vascular resistance (see above) in these challenging cases.

CMR is inferior to echo generally for the assessment of stenotic lesions. This is because the velocity profile across a stenosis is rapidly changing and a high temporal resolution is required to catch peak velocity. Although there are technical tricks possible to improve CMR temporal resolution (by decreasing 'views per segment'), this comes at the expense of longer breath holds, and a move to free breathing with multiple averages may be necessary. Since this can produce rather blurred images, many centres refrain from doing this. As a consequence the peak velocity across a stenosis (and therefore the derivative, peak gradient) is often underestimated by CMR compared to echo. Both CMR and echo may also underestimate the severity of a stenosis due to collateral run-off. A classic example of this is tight coarctation of the aorta where the peak gradient may be lower than expected due to the presence of large collateral vessels, which circumvent the obstruction and reduce the measured gradient (Fig. 4). Here, the presence of multiple large collaterals and direct inspection of the severity of the stenosis may be a better guide to its true significance than relying upon a number produced by any technique! Technical factors relating to correct implementation of phase-contrast CMR techniques are nicely reviewed by Nayak et al. (2015).

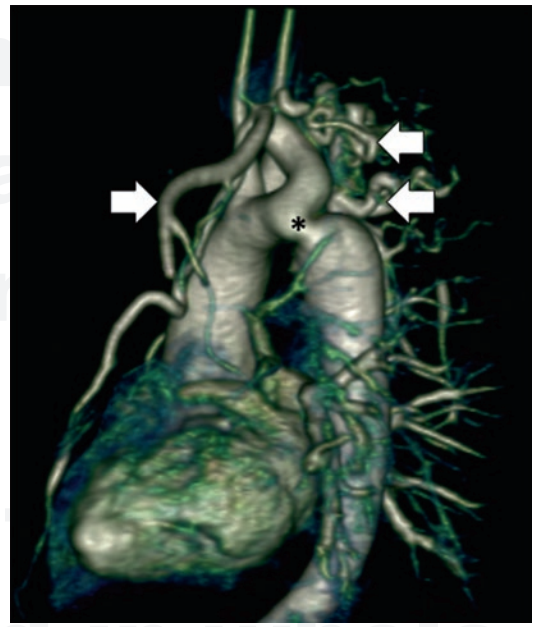

Fig. 4 Underestimation of coarctation gradient due to collateral flow. In cases of significant coarctation, it is possible for echocardiography to underestimate the severity of coarctation if run-off down large collateral vessels (arrows) means that the volume of flow across the coarct segment (asterisk), and therefore its velocity, is reduced. One way of recognising this is by using phase-contrast imaging to measure the flow in the aorta at two levels—firstly, just beyond the coarct and, secondly, at the level of the diaphragm. A significant increase in measured flow between these two points implies that there is significant collateral return to the descending aorta

There is a limited role for nuclear techniques particularly for the calculation of relative pulmonary flow in the setting of pulmonary artery stenosis. A ratio of greater than 70:30 between the two sides is usually regarded as an indication to intervene. Although this could be easily measured by CMR, there may be situations where claustrophobia or device contraindications preclude this (Roman et al. 2005). Prior stent implantation would also make direct measurement of branch flow impossible as the presence of metal disturbs the homogeneity of the magnetic field and leads to inaccurate values. CT has little or no role since flow measurement is not possible, but it may be useful to delineate areas of potential narrowing invisible to MRI—for example, within stents in the aorta or pulmonary arteries. CT may also be relevant to reveal the underlying cause of stenosis—for example, calcified homograft conduits where the obstructing calcium is low signal and difficult to recognize by CMR but readily apparent on CT (Fig. 5).

Cardiac catheterization remains the standard of reference for stenotic lesions (McLaughlin et al. 2006). The ability to measure simultaneous pressures at two distinct ends of a stenosis provides the most accurate assessment of stenosis severity. As mentioned above, lesions which appear severely stenotic on CMR or echo may be less impressive at catheterization. Many surgical decisions are still made primarily on the basis of catheter-derived gradients, and relatively few

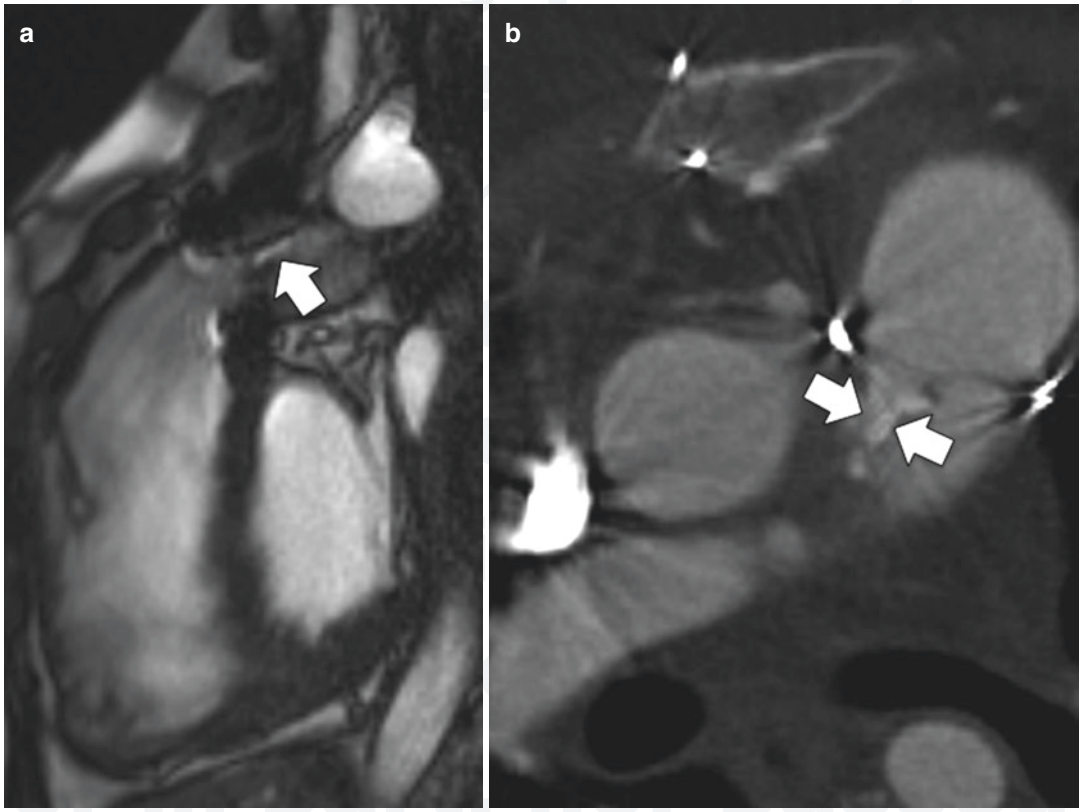

Fig. 5 Outflow tract obstruction across a homograft conduit in tetralogy of Fallot recognized by complementary imaging modalities. This patient with prior insertion of a pulmonary valve homograft conduit was noted to have increased velocities across the RVOT at echocardiography, but the exact level of obstruction could not be determined with certainty. (**a**) Sagittal cine SSFP CMR image demonstrates flow acceleration (arrow) which appears to be arising just above the level of the conduit valve. (**b**) Axial cardiac CT slice confirms that the obstruction is at valve level and is due to dystrophic calcification of both valve leaflets (arrows)

cardiologists would feel comfortable sending a patient for surgery on the basis of echo or CMR measurements alone. Measurement of shunt fraction may also be made by catheterization using the Fick principle. This assumes that flow can be derived from oxygen consumption divided by the arteriovenous difference in oxygen content of the blood. Although this is commonly done—and is reasonably accurate—it is important to understand one potential source of error is the term for oxygen consumption which is routinely *assumed* for convenience based on gender, age and body surface area rather than being directly *measured* which is preferable but more complex. Use of catheterization for assessment of regurgitant lesions is purely visual and rather dependent on operator experience.

6 Imaging Perfusion

Assessment of the coronary circulation is more commonly required than might be expected in young people in the congenital clinic. Although there are only a number of patients with coronary anomalies who present to congenital clinics each year, there are also significant numbers of patients with either inflammatory coronary disease (Kawasaki, Takayasu, Behcet) or surgical procedures which have necessitated detachment then reimplantation of the coronary arteries during surgery. Aortic root replacement, the Ross procedure and the arterial switch operation are all good examples of the latter and consequently require long-term coronary surveillance. Similarly, late presentations of coarctation are often associated with hypertension and an accelerated risk of coronary atherosclerosis which will need to be excluded prior to decision about the best treatment for the coarctation itself (Fig. 6).

There is really no consensus about the optimum approach to this sort of patient. The guidelines are vague and unhelpful in this regard. There is lack of clarity and agreement as to frequency of surveillance and modality to be used. In the absence of clear guidelines, choice of strategy may depend mainly on local imaging availability and expertise. The principal decision for the clinician is whether to seek to reassure him/herself that the myocardium is properly perfused under stress or whether to undertake direct inspection of the coronary vessels. The decisions are often—but not always—mutually exclusive as we review below.

Stress echo is an excellent modality for providing reassurance—especially when combined with treadmill stress. Most young adults are capable of reaching target heart rate, and additional prognostic data is derived from the ECG and exercise capacity portions of the test as well as the principal focus on wall motion. The test is widely available and the equipment required is inexpensive. Furthermore the lack of ionizing radiation makes it ideal for repeated examinations in a young population. The principal disadvantage stems as always from the requirement for an adequate echo window, which is variable from subject to subject. With good windows, however, a negative exercise echo can be highly reassuring.

Nuclear cardiology perfusion techniques have dominated the assessment of ischaemia in congenital patients until relatively recently. Single-photon computed emission tomography (SPECT) cameras are commonplace, and stress perfusion of the heart is easy to perform and well tolerated by patients. The main drawbacks of the technique include the associated radiation dose, which currently is in the range of 10–15 mSv using technetium isotopes (but historically was much higher with thallium isotopes). The other principal limitation of SPECT imaging is that of relatively poor spatial resolution, often in the region of 8–10 mm, which contrasts unfavourably with the 1.5–2 mm resolution achievable by CMR.

Recent advances in camera technology continue to reduce the expected dose, and with the advent of rubidium positron emission tomography (PET) imaging, doses as low as 2–4 mSv can be expected. Heavy water PET has been used on occasion and is an ideal tracer because of a linear relationship between uptake and perfusion (Yoshinaga et al. 2003; Furuyama et al. 2003, 2002). PET technology is currently limited to major academic centres however.

As PET becomes more widespread, it is likely to play a major role in the assessment of all forms of coronary disease including congenital problems. This is because of the ability to image the coronary

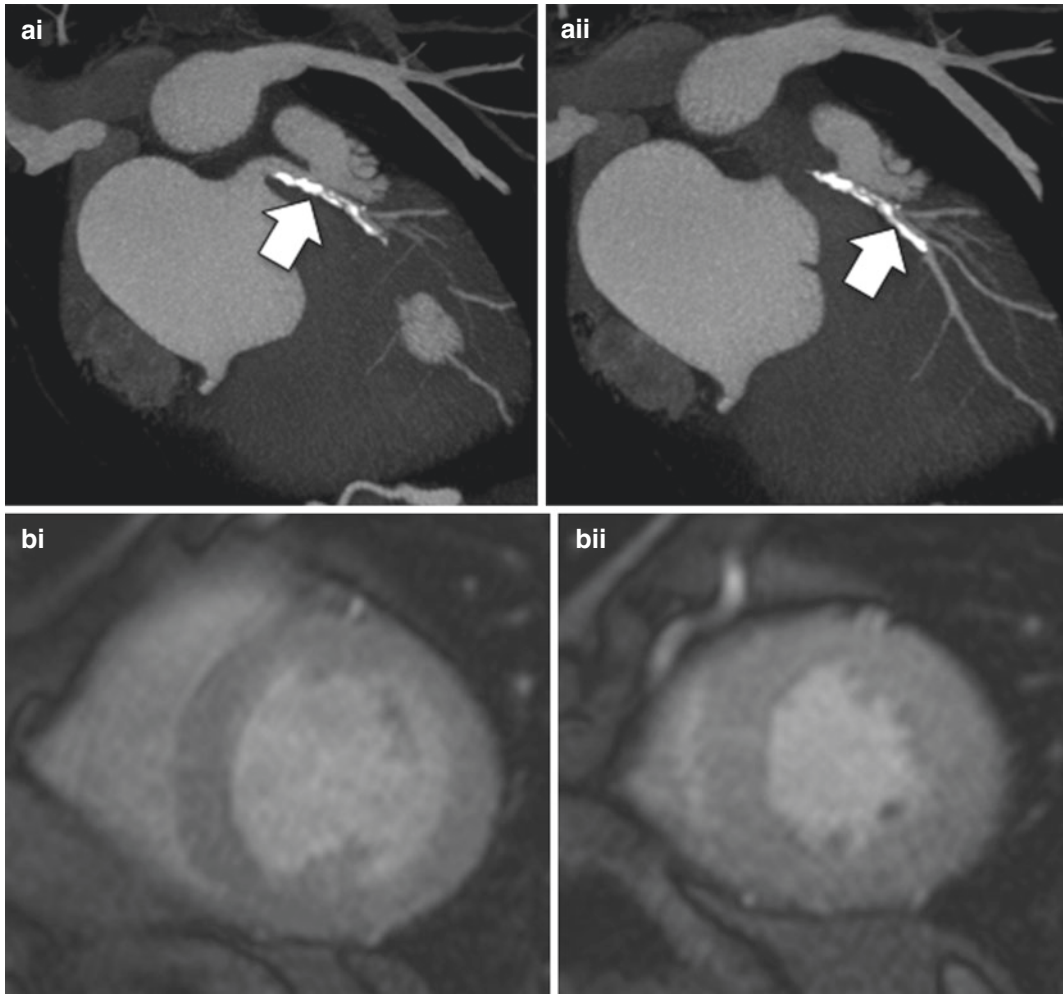

Fig. 6 Multimodality coronary imaging in a 35-year-old man with unrepaired coarctation. (**a**i–ii) Thin-slice maximum intensity projection images from cardiac CT show evidence of severe calcification of the left main and left anterior descending coronary arteries (arrows), raising concern for significant underlying stenosis. (**b**i–ii) Basal and mid-ventricular short axis slices acquired during vasodilator stress perfusion CMR, however, demonstrate normal perfusion in all coronary territories. Conventional angiography confirmed the absence of any flow-limiting coronary lesion

anatomy directly (most PET now is performed on integrated PET-CT systems) and superimpose regional flow onto three models of the vascular territories. Furthermore, software packages now allow for derivation of fully quantitative myocardial perfusion in mL/min/g of tissue, improving the specificity of the test (Hagemann et al. 2015).

PET therefore is arguably the ideal test for congenital coronary imaging despite the modest associated radiation burden. However its limited availability means that, in most large ACHD centres, CMR is regarded as the current non-invasive gold standard for perfusion assessment. The technique of vasodilator stress perfusion CMR is quick, easy and safe and has been validated extensively in adult ischaemic disease (Greenwood et al. 2009, 2012, 2014, 2016; Foley et al. 2017) and to a lesser degree in congenital heart disease. Furthermore, the use of free-breathing SSFP sequences has made it possible to acquire high-resolution images of the coronary arteries and their pathology. This has been particularly successful when applied to Kawasaki disease and congenital coronary anomalies (Fig. 7) (Tobler et al. 2014; Deva et al. 2014).

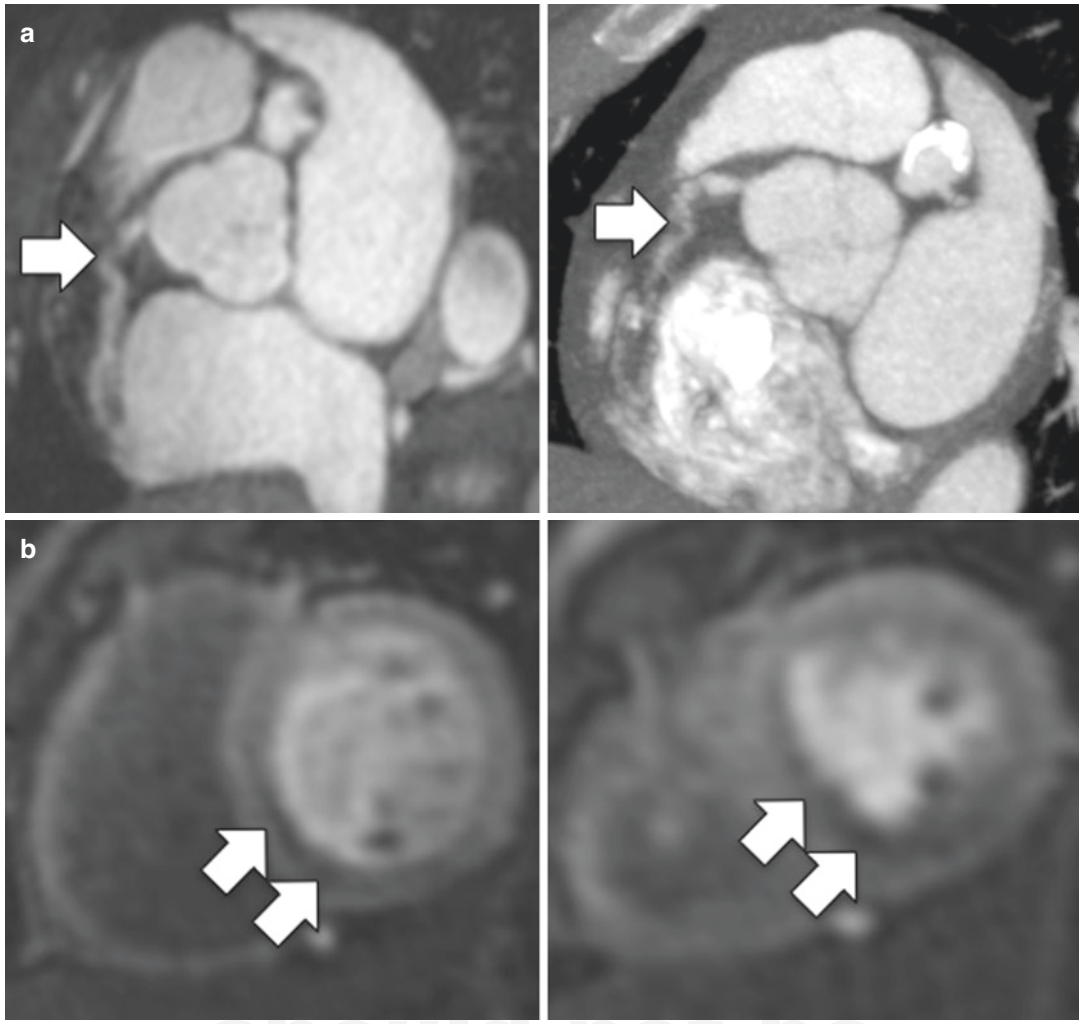

Fig. 7 Kawasaki disease with RCA occlusion. (**a**) Short axis view of the RCA (arrow) on MR angiography (left panel) and cardiac CT (right panel)—the vessel does not look entirely normal on MRA, but the extent of disease is more easily recognized on CT due to inherently higher spatial resolution. (**b**) Basal and mid-ventricular frames from vasodilator stress perfusion CMR demonstrate a zone of hypoperfusion in the inferior septum (arrows)

7 Imaging Myocardial Substrate

Patients with congenital heart disease often have abnormal myocardium. This may be congenital, for example, left ventricular non-compaction (Vermeer et al. 2013; Stähli et al. 2013; Bagur et al. 2008); or it may be acquired, for example, after chronic ischaemia or chronic volume loading. The ability to recognize and categorize abnormal myocardium has been relatively under-explored in the past in ACHD cohorts; however recent developments in the field of both molecular and CMR imaging indicate that greater attention to this area is warranted.

Substrate imaging in the nuclear world is limited by lack of clinical development although many interesting tracers have been developed for preclinical work. In practical terms SPECT-MIBI is the main tool for myocardial imaging. Persistent defects at stress and rest are usually indicative of scar—here, the absence of tracer acts as a 'negative signal' to identify abnormality. Unfortunately the limited spatial resolution of the technique means that important but limited or dispersed degrees of scarring may be missed entirely.

Conversely both diaphragmatic motion and body habitus may result in false positive defects that are misconstrued as real areas of scar (Fig. 8).

CMR has emerged as the primary method for assessing myocardial structure and composition. The technique of late gadolinium enhancement (LGE) imaging (Jimenez Juan et al. 2015) has been mainstream for 15 years and has revolutionized management of cardiomyopathies in particular. When performed with care it is exquisitely sensitive and can detect as little as 1 g of scar within the heart. In congenital work it may be used to identify areas of myocardium that have been scarred by ischaemic, mechanical or inflammatory insult (Fig. 9). It is therefore a fundamental part of any imaging protocol where coronary

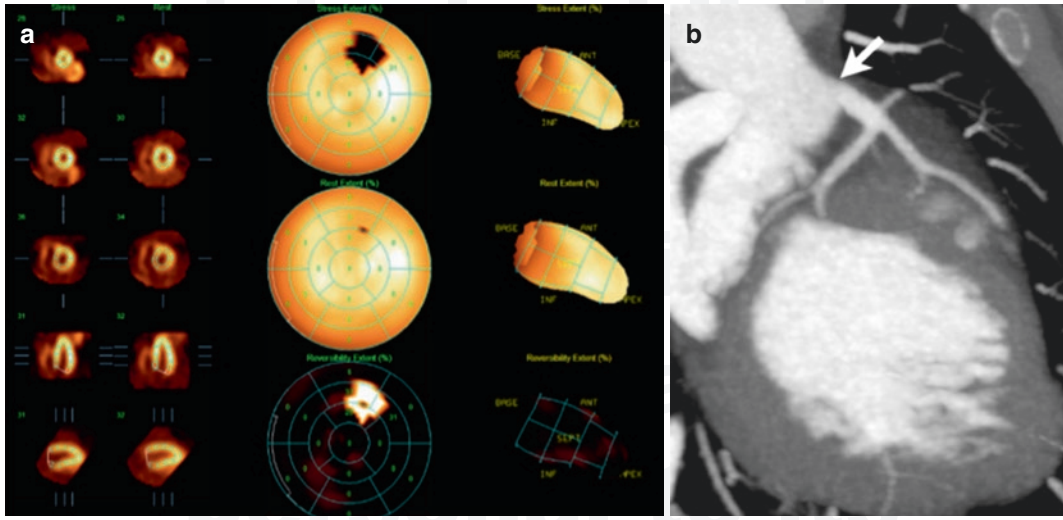

Fig. 8 False positive SPECT MIBI study in a patient following the arterial switch procedure. (**a**) Bullseye plot from stress-rest MIBI demonstrates an area of apparent reversible ischaemia in the basal to mid-anterior wall. (**b**) MIP reconstruction of the proximal to mid-left coronary tree from CT coronary angiogram demonstrates an entirely normal reimplantation site (arrow) and more distal coronary branches

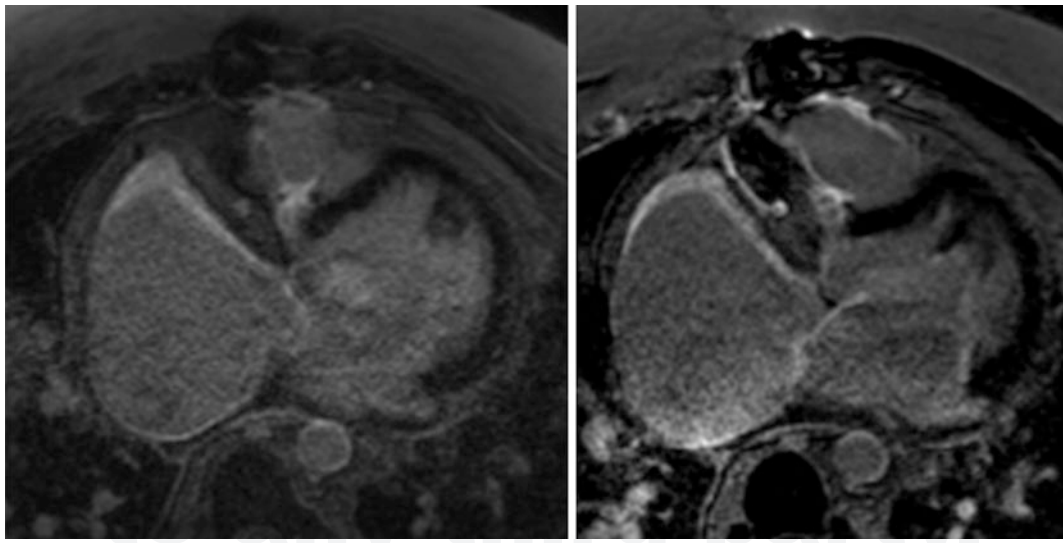

Fig. 9 Atrial fibrosis and enhancement in an atriopulmonary Fontan connection. Axial LGE images demonstrating intense enhancement in the wall of the hugely dilated right atrium. Scar in the atrial wall is common in Fontan patients but often goes unrecognized

abnormality is suspected. The very high achievable spatial resolution also makes it possible to see pathology that previously was only identifiable at surgery, for example, endocardial fibroelastosis in chronically pressure-overloaded or ischaemic ventricles (Fig. 10).

One limitation of the LGE technique, however, is the necessity for there to be some recognizable normal myocardium in the slice acquired. This is because the technique works by suppression of signal from (operator recognized) normal myocardium so that scar may be highlighted. This works well in conditions of regionality where scar is, for example, confined to a vascular territory; however it fails when there is a field change with diffuse increase in interstitial fibrosis throughout the myo-

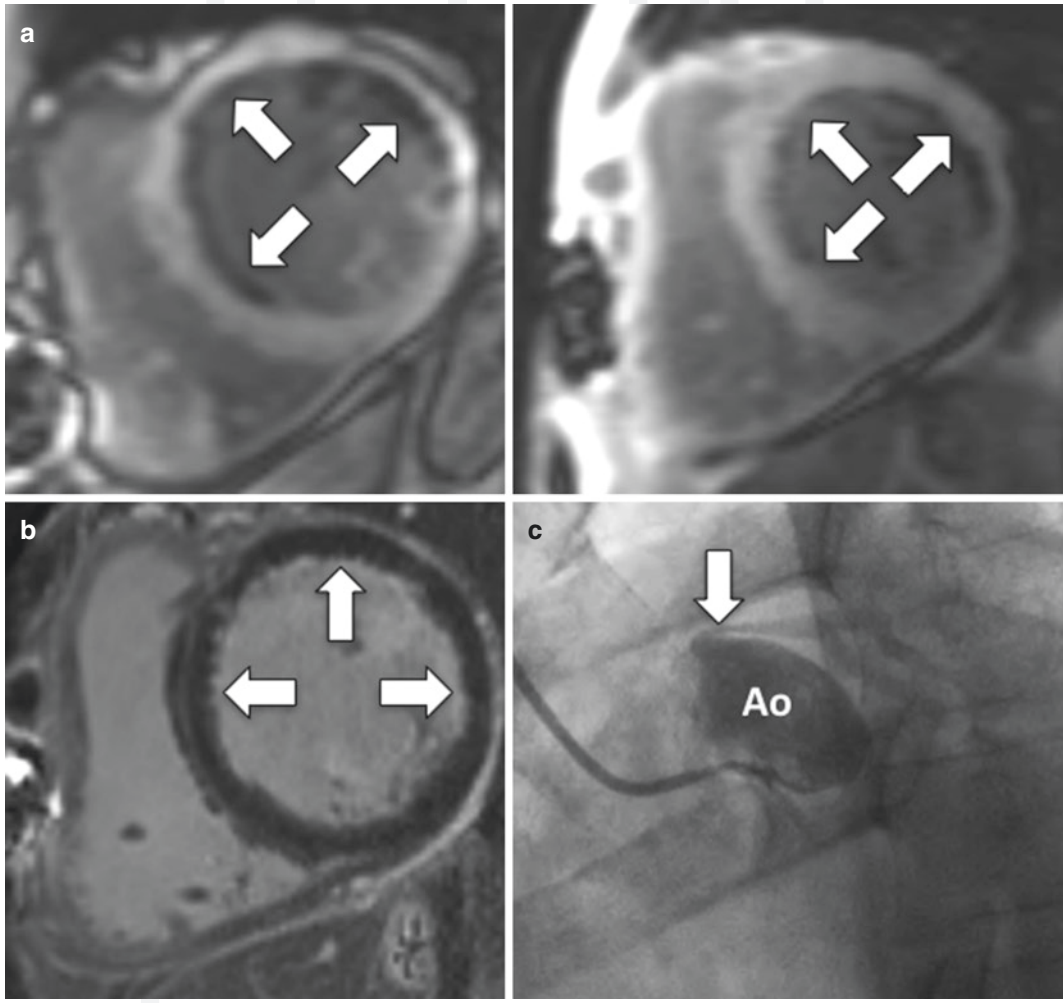

Fig. 10 Endocardial fibroelastosis (EFE) in setting of chronic ischaemia. (**a**) Basal and mid-ventricular short axis slices from an inversion time scout sequence. The majority of the myocardium is grey/white, but note the subendocardial dark rim (arrows) which has a different inversion time since it is composed of fibroelastic tissue rather than myocardium. (**b**) Short axis LGE image demonstrating a subtle inner rim of enhancing tissue (arrows) which represents the fibroelastic membrane. Very high-quality imaging is required to identify this finding—both high spatial resolution and appropriately timed image acquisition. Had LGE images been acquired even a few minutes earlier after contrast injection, the blood pool signal would have been sufficiently high to conceal the increased subendocardial signal. (**c**) Aortic root (Ao) angiogram in a man with chronic severe stenosis of the left main coronary artery (arrow) following earlier complicated reinsertion. Chronic ischaemia was believed to be the cause of the endocardial fibroelastosis in this case

cardium. More recently the technique of T1 mapping has been proposed to overcome this limitation. The details are beyond the scope of this chapter, and several useful reviews are provided (Messroghli et al. 2017; Radenkovic et al. 2017). In essence however it is possible to derive a T1 value for every pixel in the image—where the shortening of T1 post gadolinium generally reflects a local increase in fibrosis concentration. As such, a 'map' of the fibrosis content and distribution may systematically be created (Fig. 11). There are a number of assumptions made by T1 mapping, and in an attempt to reduce the influence of these, the field has lately turned towards using measured T1 values pre- and post-contrast, corrected for haematocrit, to produce instead a map of the extracellular volume (ECV) (Cameron et al. 2017; Haaf et al. 2016). In chronic conditions, the ECV corresponds mainly to the degree of interstitial fibrosis, and the normal range is 20–30% with most normal volunteers lying around 25%. Limited initial work suggests that this concept may translate to the ACHD population although it remains unclear as yet precisely how it might affect management (Hanneman et al. 2017). One possibility, however, is that subclinical heart failure—a growing problem in ACHD populations—might be detected earlier through an ECV biomarker than by conventional measures such as ejection fraction (Riesenkampff et al. 2015; Schelbert et al. 2015).

8 Imaging Thrombus

Thrombus is usually a result of derangement of one or more of the three principal components of Virchow's triad:

- Altered coagulability
- Altered wall
- Altered flow

This is not a trivial issue in adult congenital heart disease as many patients will have two if not three of these conditions. Fontan patients are peculiarly vulnerable to developing thrombus particularly if they have one of the older right atrium to pulmonary artery type connections (RA-PA Fontan) (Fig. 12). These—often very dilated—chambers with swirling flow provide ideal conditions for thrombus to form and possibly embolize more distally within the circulation (Fig. 13). Atrial arrhythmias may compound the thrombotic tendency. This kind of event may be life-threatening in a Fontan patient, and prompt recognition and treatment of this complication are vital.

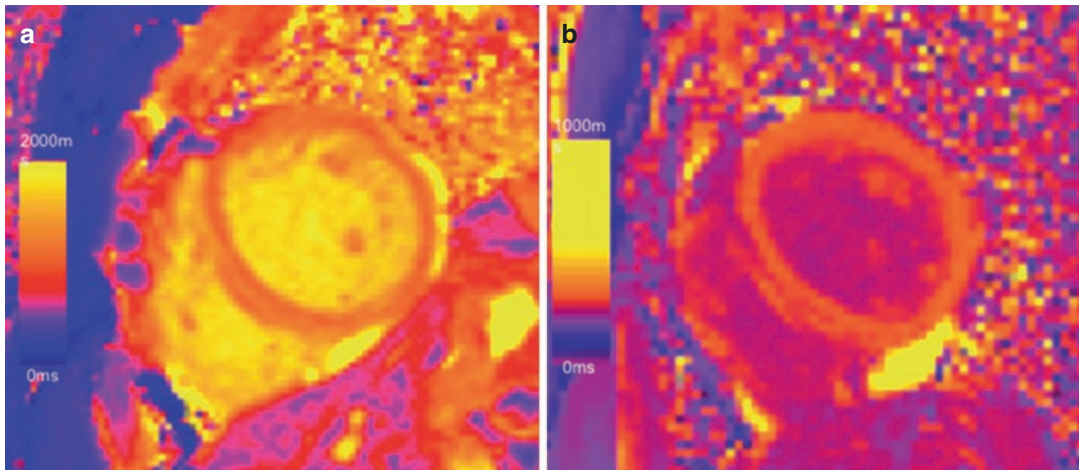

Fig. 11 T1 mapping in congenital heart disease. Adult patient with unrepaired anomalous left coronary artery from the pulmonary artery. (**a**) Native (pre-contrast) T1 map. (**b**) Post-contrast T1 map. Combined, these maps allow generation of an extracellular volume (ECV) map which—in the chronic situation—reflects the degree of underlying diffuse tissue fibrosis. Normal ECV is 20–30%. This patient has an ECV of about 32% even though the LGE imaging was unremarkable—and as such may be a more sensitive marker for diffuse tissue changes

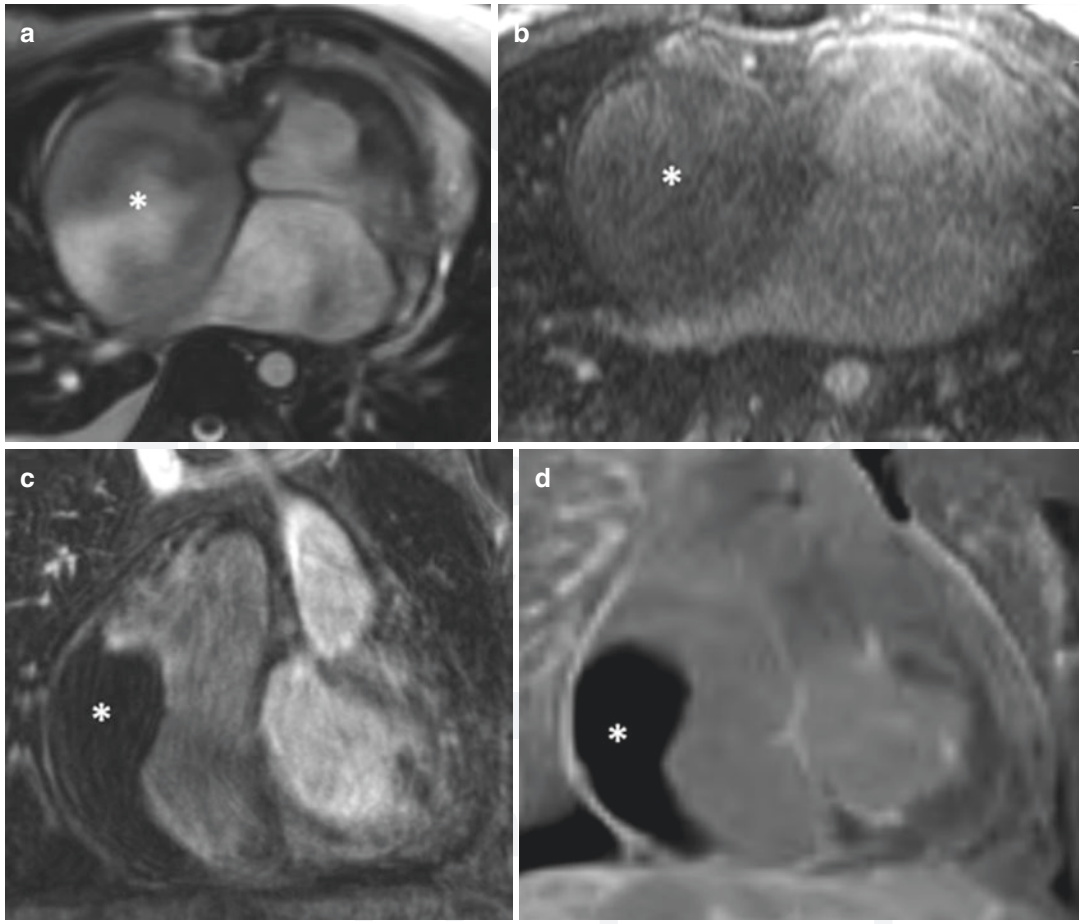

Fig. 12 The challenges of identifying thrombus in ACHD patients. (**a**) Axial cine SSFP image demonstrates mixed intensities suspicious for thrombus in the right atrium (asterisk) in this patient with a Fontan circuit. (**b**) Same patient following contrast—no thrombus is present. The appearances in (**a**) were due to swirling slow flow only. (**c**) Same patient several years later with thrombus (asterisk) visible in the right atrium on coronal view from MR angiogram. (**d**) This is made even more obvious by using phase-sensitive inversion recovery LGE sequences—with thrombus (asterisk) appearing uniformly low signal

Echo is usually the first-line examination for such a patient. In our experience transthoracic echo rarely allows confident exclusion of thrombus within a Fontan circuit. More surprising is how often transesophageal echocardiography leads to an equivocal 'unable to definitively rule out thrombus'. Why does echo find it so difficult? The answer lies in the appearance of slow-moving twisting patterns of blood flow giving rise to what echocardiographers refer to as 'smoke' within the atrium. In places this smoke may be sufficiently dense and slow moving as to be indistinguishable from fully formed thrombus. A similar phenomenon can be seen in the giant aneurysms of Kawasaki patients in whom swirling flow is problematic and can even confuse at the time of coronary angiography.

CMR suffers from the same limitation when only cine imaging is used for assessment. However, after administration of gadolinium, the use of LGE imaging invariably allows confident detection or exclusion of thrombus (Srichai et al. 2006; Goyal and Weinsaft 2013). This is because LGE imaging is usually performed 8–10 min after the administration of contrast by which time even the slow-moving currents of flow within the right atrium have had chance to distribute the gadolinium evenly throughout the chamber (Fig. 12).

Patients who are unwell and unstable or who have a contraindication to CMR may be alternatively

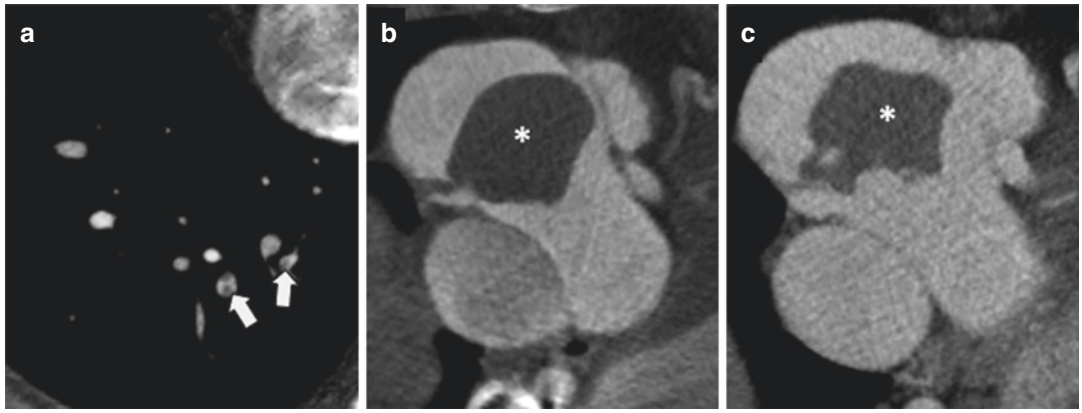

Fig. 13 Cardiac CT to identify thrombus in a Fontan patient. (**a**) The patient presented with acute breathlessness, and CT pulmonary angiogram demonstrated right lower lobe filling defects (arrows) consistent with pulmonary emboli. (**b**) Axial CT image with large low attenuation mass (asterisk) in the right atrium, consistent with thrombus and attached by a thin stalk to the posterior atrial wall. (**c**) Same patient 1 month later after anticoagulation. The thrombus is still present (asterisk) but has reduced in size. Cardiac CT is a very rapid method for identifying thrombus in the heart and can be performed at very low radiation doses by use of a low-kilovoltage technique

investigated by cardiac CT (Fig. 13). This is an excellent modality for thrombus detection aided by best-in-class spatial resolution and unlimited multiplanar reconstruction abilities (Choi et al. 2017). Many modern scanners have dual-energy capability which may further enhance discrimination between slow-flowing blood and genuine thrombus (Hur et al. 2012). Although dose has been a concern in the past, an examination of diagnostic quality can be carried out at a dose of only 1–2 mSv or even less if dose factors are aggressively modulated. Since we see many patients with atrial arrhythmias related to a variety of underlying lesions, it would be challenging to arrange CMR rapidly in each case prior to cardioversion. Over the years we have increasingly moved away from pre-cardioversion transesophageal echo and now perform cardiac CT instead in many cases—transforming both the workflow and the patient experience—with no adverse outcomes.

9 Imaging Infection

Imaging infection in ACHD usually means imaging endocarditis, which is unfortunately not a rare occurrence in this population (Li and Somerville 1998). Here there is no doubt that echocardiography—both transthoracic and transesophageal—comes into its own (Greaves et al. 2003). Detection of vegetations may be challenging if small and rapidly moving and only echo really has sufficient spatial and temporal resolution to do this reliably. There is little role for CMR here, except perhaps occasionally to confirm embolism from an aortic valve vegetation—by demonstration of new oedema and scar in a coronary territory or by revealing acute cerebral embolic lesions.

CT, however, has a more relevant role. Right-sided (tricuspid, pulmonary) lesions should routinely undergo periodic surveillance to ensure that silent pulmonary embolism is not occurring with risk for empyema and mycotic aneurysm formation. Left-sided lesions—particularly aortic—should probably undergo baseline screening once the diagnosis is established with imaging of the brain, chest, abdomen and pelvis to establish the event of embolic disease in case there is later deterioration, which might then favour surgery. Infection that is slow to respond with persistent fever and/or elevation of inflammatory markers should prompt a search for occult sources (Fig. 14).

A more recent addition to the imaging armamentarium for endocarditis is FDG PET imaging (Pizzi et al. 2015). This has been shown to be effective in whole-body screening of patients to

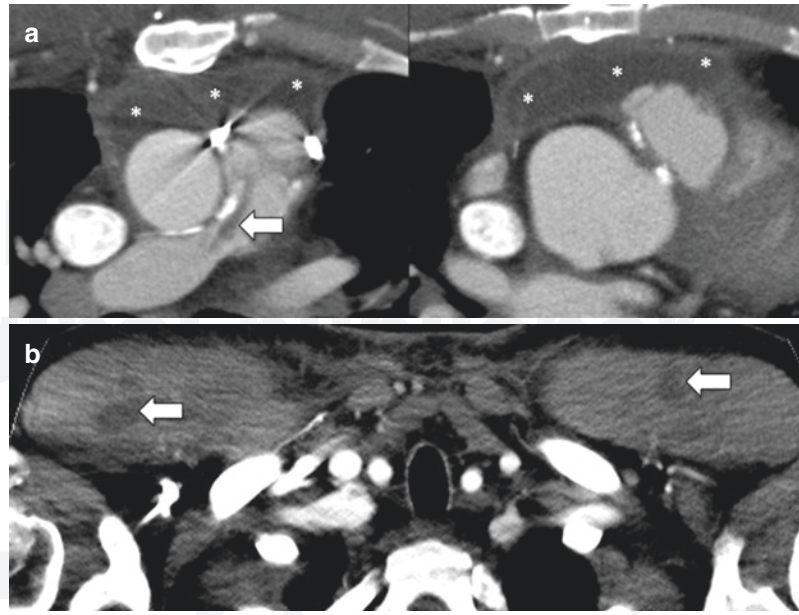

Fig. 14 Detection of disseminated infection in endocarditis. (**a**) Axial post-contrast CT image in a patient with pulmonary valve homograft endocarditis (arrow) and an anterior mediastinal collection (asterisks) with a thickened enhancing wall. (**b**) Incidental detection of multiple pectoral muscle abscesses (arrows) in the same patient

look for evidence of unsuspected embolism to various vascular beds (Amraoui et al. 2016; Bonfiglioli et al. 2013; Van Riet et al. 2010). It also enables early reclassification from possible endocarditis to a definite or rejected diagnosis of endocarditis. Although available literature is principally confined to non-ACHD patients, there are early data suggesting that this might be equally valuable in congenital heart patients, many of whom have prosthetic valves and devices (Pizzi et al. 2017). Since FDG imaging may be performed even on standard SPECT cameras equipped with appropriate collimators, this may become a more widespread approach in the future.

10 Imaging Surgical Complications

Complications following surgery for ACHD are an unfortunate fact of life. Prompt recognition of a problem by a surgeon is usually followed by an equally prompt request for imaging! There is no substitute for talking directly to the surgeon in order to find out what (s)he did at the operation and what (s)he feels may have gone wrong. This is essential in order to tailor the examination to the precise question of concern. Failure to do this usually results in requests for additional imaging in subsequent days.

No specific guidance can be given in this section since the imaging required varies according to situation. A few general comments may be made. Cardiac MR is usually poorly tolerated in the immediate post-operative period, and image quality is often poor. It may be useful however if there are concerns about myocardial damage. Cardiac CT is a very rapid and well-tolerated examination even in quite sick patients and may provide a lot of information above and beyond what may be obtained by echocardiography (although the two are usually complementary). If a surgeon is concerned about coronary artery compromise (ECG or wall motion abnormality or unexpected troponin rise), it is rare that anything other than a conventional coronary angiogram will reassure. However, following a normal angiogram, CMR may reveal the cause for chest pain.

11 Imaging by Invasive Coronary Angiography

Despite the bias towards non-invasive imaging in this chapter, it should be recognized that coronary catheterization is neither outdated nor irrelevant. Imaging in its broader sense also includes physiologic imaging, and the determination of intracardiac pressures is of vital importance both for diagnosis and management. Likewise for an experienced operator, there is little substitute for an angiographic roadmap and measurements derived from catheter images. Conventional angiographers are increasingly interested in seeing how the 3D data derived from CT and CMR may be integrated with the angiographic data to plan procedures such as coarctation stenting and pulmonary valve implantation. Coronary angiography remains the gold standard for the assessment of chest pain in general ACHD patients and is specifically indicated in most congenital patients with coronary anomalies of origin, course and termination—particularly when associated with symptoms. Direct arterial injection permits the visualization of flow within coronary arteries, fistulae and aneurysms in a way that remains impossible for CT and CMR. For coronaries with an intramural proximal course, the possibility of physiologic assessment by fractional flow reserve and intravascular ultrasound arises. More recently optical coherence tomography has also been employed to look at the structure of the coronary wall in conditions such as Kawasaki disease.

Conclusion

Adult congenital heart disease is a challenging area in which to work. No two patients are alike—even those who appear to share a common underlying lesion. The temporal evolution of surgery and intervention means that patients born 40 years ago may look quite different from those born 20 years ago even if they share the same diagnosis. The variety and complexity amongst the ACHD population argues for a personalized rather than dogmatic approach to imaging. Flexibility of approach—and sometimes more than one approach—is needed to fully characterize the challenging lesions and problems seen in this population.

References

Alfakih K, Plein S, Thiele H, Jones T, Ridgway JP, Sivananthan MU (2003a) Normal human left and right ventricular dimensions for MRI as assessed by turbo gradient echo and steady-state free precession imaging sequences. J Magn Reson Imaging 17(3):323–329

Alfakih K, Plein S, Bloomer T, Jones T, Ridgway J, Sivananthan M (2003b) Comparison of right ventricular volume measurements between axial and short axis orientation using steady-state free precession magnetic resonance imaging. J Magn Reson Imaging 18(1):25–32

Amraoui S, Tlili G, Sohal M, Berte B, Hindié E, Ritter P et al (2016) Contribution of PET imaging to the diagnosis of septic embolism in patients with pacing lead endocarditis. JACC Cardiovasc Imaging 9(3):283–290

Bagur RH, Lederlin M, Montaudon M, Latrabe V, Corneloup O, Iriart X et al (2008) Images in cardiovascular medicine. Ebstein anomaly associated with left ventricular noncompaction. Circulation 118(16):e662–e664

Bonfiglioli R, Nanni C, Morigi JJ, Graziosi M, Trapani F, Bartoletti M et al (2013) ^{18}F-FDG PET/CT diagnosis of unexpected extracardiac septic embolisms in patients with suspected cardiac endocarditis. Eur J Nucl Med Mol Imaging 40(8):1190–1196

Buechel EV, Kaiser T, Jackson C, Schmitz A, Kellenberger CJ (2009) Normal right- and left ventricular volumes and myocardial mass in children measured by steady state free precession cardiovascular magnetic resonance. J Cardiovasc Magn Reson 11:19

Cain PA, Ahl R, Hedstrom E, Ugander M, Allansdotter-Johnsson A, Friberg P et al (2009) Age and gender specific normal values of left ventricular mass, volume and function for gradient echo magnetic resonance imaging: a cross sectional study. BMC Med Imaging 9:2

Cameron D, Vassiliou VS, Higgins DM, Gatehouse PD (2017) Towards accurate and precise T1 and extracellular volume mapping in the myocardium: a guide to current pitfalls and their solutions. MAGMA. https://doi.org/10.1007/s10334-017-0631-2

Celermajer DS, Greaves K (2002) Survivors of coarctation repair: fixed but not cured. Heart 88(2):113–114

Childs H, Ma L, Ma M, Clarke J, Cocker M, Green J et al (2011) Comparison of long and short axis quantification of left ventricular volume parameters by cardio-

vascular magnetic resonance, with ex-vivo validation. J Cardiovasc Magn Reson 13:40

Choi YR, Kim H-L, Kwon H-M, Chun EJ, Ko SM, Yoo SM et al (2017) Cardiac CT and MRI for assessment of cardioembolic stroke. Cardiovasc Imaging. Asia 1(1):13

Clay S, Alfakih K, Radjenovic A, Jones T, Ridgway JP, Sinvananthan MU (2006) Normal range of human left ventricular volumes and mass using steady state free precession MRI in the radial long axis orientation. MAGMA 19(1):41–45

Crean AM, Maredia N, Ballard G, Menezes R, Wharton G, Forster J et al (2011) 3D Echo systematically underestimates right ventricular volumes compared to cardiovascular magnetic resonance in adult congenital heart disease patients with moderate or severe RV dilatation. J Cardiovasc Magn Reson 13:78

DeFaria Yeh D, Foster E (2014) Is MRI the preferred method for evaluating right ventricular size and function in patients with congenital heart disease?: MRI is not the preferred method for evaluating right ventricular size and function in patients with congenital heart disease. Circ Cardiovasc Imaging 7(1):198–205

Deva DP, Torres FS, Wald RM, Roche SL, Jimenez-Juan L, Oechslin EN et al (2014) The value of stress perfusion cardiovascular magnetic resonance imaging for patients referred from the adult congenital heart disease clinic: 5-year experience at the Toronto General Hospital. Cardiol Young 24(5):822–830

Foley JRJ, Kidambi A, Biglands JD, Maredia N, Dickinson CJ, Plein S et al (2017) A comparison of cardiovascular magnetic resonance and single photon emission computed tomography (SPECT) perfusion imaging in left main stem or equivalent coronary artery disease: a CE-MARC substudy. J Cardiovasc Magn Reson 19(1):84

Fratz S, Schuhbaeck A, Buchner C, Busch R, Meierhofer C, Martinoff S et al (2009) Comparison of accuracy of axial slices versus short-axis slices for measuring ventricular volumes by cardiac magnetic resonance in patients with corrected tetralogy of fallot. Am J Cardiol 103(12):1764–1769

Fuchs A, Mejdahl MR, Kühl JT, Stisen ZR, Nilsson EJP, Køber LV et al (2016) Normal values of left ventricular mass and cardiac chamber volumes assessed by 320-detector computed tomography angiography in the Copenhagen General Population Study. Eur Heart J Cardiovasc Imaging 17(9):1009–1017

Furuyama H, Odagawa Y, Katoh C, Iwado Y, Yoshinaga K, Ito Y et al (2002) Assessment of coronary function in children with a history of Kawasaki disease using (15)O-water positron emission tomography. Circulation 105(24):2878–2884

Furuyama H, Odagawa Y, Katoh C, Iwado Y, Ito Y, Noriyasu K et al (2003) Altered myocardial flow reserve and endothelial function late after Kawasaki disease. J Pediatr 142(2):149–154

Garcia-Bournissen F, Shrim A, Koren G (2006) Safety of gadolinium during pregnancy. Can Fam Physician 52:309–310

Geva T (2014) Is MRI the preferred method for evaluating right ventricular size and function in patients with congenital heart disease?: MRI is the preferred method for evaluating right ventricular size and function in patients with congenital heart disease. Circ Cardiovasc Imaging 7(1):190–197

Goyal P, Weinsaft JW (2013) Cardiovascular magnetic resonance imaging for assessment of cardiac thrombus. Methodist Debakey Cardiovasc J 9(3):132–136

Greaves K, Mou D, Patel A, Celermajer DS (2003) Clinical criteria and the appropriate use of transthoracic echocardiography for the exclusion of infective endocarditis. Heart 89(3):273–275

Greenwood JP, Maredia N, Radjenovic A, Brown JM, Nixon J, Farrin AJ et al (2009) Clinical evaluation of magnetic resonance imaging in coronary heart disease: the CE-MARC study. Trials 10:62

Greenwood JP, Maredia N, Younger JF, Brown JM, Nixon J, Everett CC et al (2012) Cardiovascular magnetic resonance and single-photon emission computed tomography for diagnosis of coronary heart disease (CE-MARC): a prospective trial. Lancet 379(9814):453–460

Greenwood JP, Motwani M, Maredia N, Brown JM, Everett CC, Nixon J et al (2014) Comparison of cardiovascular magnetic resonance and single-photon emission computed tomography in women with suspected coronary artery disease from the Clinical Evaluation of Magnetic Resonance Imaging in Coronary Heart Disease (CE-MARC) Trial. Circulation 129(10):1129–1138

Greenwood JP, Herzog BA, Brown JM, Everett CC, Nixon J, Bijsterveld P et al (2016) Prognostic value of cardiovascular magnetic resonance and single-photon emission computed tomography in suspected coronary heart disease: long-term follow-up of a prospective, diagnostic accuracy cohort study. Ann Intern Med. https://doi.org/10.7326/M15-1801

Grosse-Wortmann L, Al-Otay A, Goo HW, Macgowan CK, Coles JG, Benson LN et al (2007) Anatomical and functional evaluation of pulmonary veins in children by magnetic resonance imaging. J Am Coll Cardiol 49(9):993–1002

Haaf P, Garg P, Messroghli DR, Broadbent DA, Greenwood JP, Plein S (2016) Cardiac T1 Mapping and Extracellular Volume (ECV) in clinical practice: a comprehensive review. J Cardiovasc Magn Reson 18(1):89

Hagemann CE, Ghotbi AA, Kjær A, Hasbak P (2015) Quantitative myocardial blood flow with Rubidium-82 PET: a clinical perspective. Am J Nucl Med Mol Imaging 5(5):457–468

Han BK, Rigsby CK, Hlavacek A, Leipsic J, Nicol ED, Siegel MJ et al (2015a) Computed tomography imaging in patients with congenital heart disease Part I: Rationale and utility. An Expert Consensus Document of the Society of Cardiovascular Computed Tomography (SCCT): Endorsed by the Society of Pediatric Radiology (SPR) and the North American

Society of Cardiac Imaging (NASCI). J Cardiovasc Comput Tomogr 9(6):475–492

Han BK, Rigsby CK, Leipsic J, Bardo D, Abbara S, Ghoshhajra B et al (2015b) Computed tomography imaging in patients with congenital heart disease, Part 2: Technical Recommendations. An Expert Consensus Document of the Society of Cardiovascular Computed Tomography (SCCT): Endorsed by the Society of Pediatric Radiology (SPR) and the North American Society of Cardiac Imaging (NASCI). J Cardiovasc Comput Tomogr 9(6):493–513

Hanneman K, Crean AM, Wintersperger BJ, Thavendiranathan P, Nguyen ET, Kayedpour C et al (2017) The relationship between cardiovascular magnetic resonance imaging measurement of extracellular volume fraction and clinical outcomes in adults with repaired tetralogy of Fallot. Eur Heart J Cardiovasc Imaging. https://doi.org/10.1093/ehjci/jex248

Harel F, Finnerty V, Ngo Q, Grégoire J, Khairy P, Thibault B (2007) SPECT versus planar gated blood pool imaging for left ventricular evaluation. J Nucl Cardiol 14(4):544–549

Hesse B, Lindhardt TB, Acampa W, Anagnostopoulos C, Ballinger J, Bax JJ et al (2008) EANM/ESC guidelines for radionuclide imaging of cardiac function. Eur J Nucl Med Mol Imaging 35(4):851–885

Hudsmith LE, Petersen SE, Francis JM, Robson MD, Neubauer S (2005) Normal human left and right ventricular and left atrial dimensions using steady state free precession magnetic resonance imaging. J Cardiovasc Magn Reson 7(5):775–782

Hur J, Kim YJ, Lee H-J, Nam JE, Hong YJ, Kim HY et al (2012) Cardioembolic stroke: dual-energy cardiac CT for differentiation of left atrial appendage thrombus and circulatory stasis. Radiology 263(3):688–695

James SH, Wald R, Wintersperger BJ, Jimenez-Juan L, Deva D, Crean AM et al (2013) Accuracy of right and left ventricular functional assessment by short-axis vs axial cine steady-state free-precession magnetic resonance imaging: intrapatient correlation with main pulmonary artery and ascending aorta phase-contrast flow measurements. Can Assoc Radiol J 64(3):213–219

Jimenez Juan L, Crean AM, Wintersperger BJ (2015) Late gadolinium enhancement imaging in assessment of myocardial viability: techniques and clinical applications. Radiol Clin N Am 53(2):397–411

Johnson LL, Lawson MA (1996) New imaging techniques for assessing cardiac function. Crit Care Clin 12(4):919–937

Juergens KU, Grude M, Maintz D, Fallenberg EM, Wichter T, Heindel W et al (2004) Multi-detector row CT of left ventricular function with dedicated analysis software versus MR imaging: initial experience. Radiology 230(2):403–410

Koch K, Oellig F, Kunz P, Bender P, Oberholzer K, Mildenberger P et al (2004) Assessment of global and regional left ventricular function with a 16-slice spiral-CT using two different software tools for quantitative functional analysis and qualitative evaluation of wall motion changes in comparison with magnetic resonance imaging. Röfo 176(12):1786–1793

Li W, Somerville J (1998) Infective endocarditis in the grown-up congenital heart (GUCH) population. Eur Heart J 19(1):166–173

Lorenz CH, Walker ES, Morgan VL, Klein SS, Graham TP (1999) Normal human right and left ventricular mass, systolic function, and gender differences by cine magnetic resonance imaging. J Cardiovasc Magn Reson 1(1):7–21

Lotz J, Meier C, Leppert A, Galanski M (2002) Cardiovascular flow measurement with phase-contrast MR imaging: basic facts and implementation 1. Radiographics 22(3):651–671

Maceira AM, Prasad SK, Khan M, Pennell DJ (2006) Reference right ventricular systolic and diastolic function normalized to age, gender and body surface area from steady-state free precession cardiovascular magnetic resonance. Eur Heart J 27(23):2879–2888

Mahnken AH, Spuentrup E, Niethammer M, Buecker A, Boese J, Wildberger JE et al (2003) Quantitative and qualitative assessment of left ventricular volume with ECG-gated multislice spiral CT: value of different image reconstruction algorithms in comparison to MRI. Acta Radiol 44(6):604–611

Marelli AJ, Mackie AS, Ionescu-Ittu R, Rahme E, Pilote L (2007) Congenital heart disease in the general population: changing prevalence and age distribution. Circulation 115(2):163–172

McLaughlin P, Benson L, Horlick E (2006) The role of cardiac catheterization in adult congenital heart disease. Cardiol Clin 24(4):531–556, v

Mercer-Rosa L, Yang W, Kutty S, Rychik J, Fogel M, Goldmuntz E (2012) Quantifying pulmonary regurgitation and right ventricular function in surgically repaired tetralogy of Fallot: a comparative analysis of echocardiography and magnetic resonance imaging. Circ Cardiovasc Imaging 5(5):637–643

Messroghli DR, Moon JC, Ferreira VM, Grosse-Wortmann L, He T, Kellman P et al (2017) Clinical recommendations for cardiovascular magnetic resonance mapping of T1, T2, T2* and extracellular volume: a consensus statement by the Society for Cardiovascular Magnetic Resonance (SCMR) endorsed by the European Association for Cardiovascular Imaging (EACVI). J Cardiovasc Magn Reson 19(1):75

Moody WE, Edwards NC, Chue CD, Taylor RJ, Ferro CJ, Townend JN et al (2015) Variability in cardiac MR measurement of left ventricular ejection fraction, volumes and mass in healthy adults: defining a significant change at 1 year. Br J Radiol 88(1049):20140831

Mooij CF, de Wit CJ, Graham DA, Powell AJ, Geva T (2008) Reproducibility of MRI measurements of right ventricular size and function in patients with normal and dilated ventricles. J Magn Reson Imaging 28(1):67–73

Navare SM, Wackers FJT, Liu Y-H (2003) Comparison of 16-frame and 8-frame gated SPET imaging for determination of left ventricular volumes and

ejection fraction. Eur J Nucl Med Mol Imaging 30(10):1330–1337
Nayak KS, Nielsen J-F, Bernstein MA, Markl M, Gatehouse PD, Botnar RM et al (2015) Cardiovascular magnetic resonance phase contrast imaging. J Cardiovasc Magn Reson 17(1):71
Petersen SE, Aung N, Sanghvi MM, Zemrak F, Fung K, Paiva JM et al (2017) Reference ranges for cardiac structure and function using cardiovascular magnetic resonance (CMR) in Caucasians from the UK Biobank population cohort. J Cardiovasc Magn Reson 19(1):18
Pizzi MN, Roque A, Fernández-Hidalgo N, Cuéllar-Calabria H, Ferreira-González I, Gonzàlez-Alujas MT et al (2015) Improving the diagnosis of infective endocarditis in prosthetic valves and intracardiac devices with 18F-fluordeoxyglucose positron emission tomography/computed tomography angiography: initial results at an infective endocarditis referral center. Circulation 132(12):1113–1126
Pizzi MN, Dos-Subirà L, Roque A, Fernández-Hidalgo N, Cuéllar-Calabria H, Pijuan Domènech A et al (2017) (18)F-FDG-PET/CT angiography in the diagnosis of infective endocarditis and cardiac device infection in adult patients with congenital heart disease and prosthetic material. Int J Cardiol 248:396–402
Radenkovic D, Weingärtner S, Ricketts L, Moon JC, Captur G (2017) T1 mapping in cardiac MRI. Heart Fail Rev 22(4):415–430
Riesenkampff E, Messroghli DR, Redington AN, Grosse-Wortmann L (2015) Myocardial T1 mapping in pediatric and congenital heart disease. Circ Cardiovasc Imaging 8(2):e002504
Roche SL, Silversides CK, Oechslin EN (2011) Monitoring the patient with transposition of the great arteries: arterial switch versus atrial switch. Curr Cardiol Rep 13(4):336–346
Roman KS, Kellenberger CJ, Farooq S, MacGowan CK, Gilday DL, Yoo S-J (2005) Comparative imaging of differential pulmonary blood flow in patients with congenital heart disease: magnetic resonance imaging versus lung perfusion scintigraphy. Pediatr Radiol 35(3):295–301
Salton CJ, Chuang ML, O'Donnell CJ, Kupka MJ, Larson MG, Kissinger KV et al (2002) Gender differences and normal left ventricular anatomy in an adult population free of hypertension. A cardiovascular magnetic resonance study of the Framingham Heart Study Offspring cohort. J Am Coll Cardiol 39(6):1055–1060
Schelbert HR, Verba JW, Johnson AD, Brock GW, Alazraki NP, Rose FJ et al (1975) Nontraumatic determination of left ventricular ejection fraction by radionuclide angiocardiography. Circulation 51(5):902–909
Schelbert EB, Piehler KM, Zareba KM, Moon JC, Ugander M, Messroghli DR et al (2015) Myocardial fibrosis quantified by extracellular volume is associated with subsequent hospitalization for heart failure, death, or both across the spectrum of ejection fraction and heart failure stage. J Am Heart Assoc 4(12):e002613
Sievers B, Kirchberg S, Bakan A, Franken U, Trappe H-J (2004) Impact of papillary muscles in ventricular volume and ejection fraction assessment by cardiovascular magnetic resonance. J Cardiovasc Magn Reson 6(1):9–16
Singh RM, Singh BM, Mehta JL (2014) Role of cardiac CTA in estimating left ventricular volumes and ejection fraction. World J Radiol 6(9):669–676
Srichai MB, Junor C, Rodriguez LL, Stillman AE, Grimm RA, Lieber ML et al (2006) Clinical, imaging, and pathological characteristics of left ventricular thrombus: a comparison of contrast-enhanced magnetic resonance imaging, transthoracic echocardiography, and transesophageal echocardiography with surgical or pathological validation. Am Heart J 152(1):75–84
Stähli BE, Gebhard C, Biaggi P, Klaassen S, Valsangiacomo Buechel E, Attenhofer Jost CH et al (2013) Left ventricular non-compaction: prevalence in congenital heart disease. Int J Cardiol 167(6):2477–2481
Stehning C, Börnert P, Nehrke K, Eggers H, Stuber M (2005) Free-breathing whole-heart coronary MRA with 3D radial SSFP and self-navigated image reconstruction. Magn Reson Med 54(2):476–480
Strugnell WE, Slaughter IR, Riley RA, Trotter AJ, Bartlett H (2005) Modified RV short axis series—a new method for cardiac MRI measurement of right ventricular volumes. J Cardiovasc Magn Reson 7(5):769–774
Sundgren PC, Leander P (2011) Is administration of gadolinium-based contrast media to pregnant women and small children justified? J Magn Reson Imaging 34(4):750–757
Tobler D, Motwani M, Wald RM, Roche SL, Verocai F, Iwanochko RM et al (2014) Evaluation of a comprehensive cardiovascular magnetic resonance protocol in young adults late after the arterial switch operation for d-transposition of the great arteries. J Cardiovasc Magn Reson 16:98
Van Riet J, Hill EE, Gheysens O, Dymarkowski S, Herregods M-C, Herijgers P et al (2010) (18)F-FDG PET/CT for early detection of embolism and metastatic infection in patients with infective endocarditis. Eur J Nucl Med Mol Imaging 37(6):1189–1197
Vermeer AMC, van Engelen K, Postma AV, Baars MJH, Christiaans I, De Haij S et al (2013) Ebstein anomaly associated with left ventricular noncompaction: an autosomal dominant condition that can be caused by mutations in MYH7. Am J Med Genet C: Semin Med Genet 163C(3):178–184
Winter MM, Bernink FJ, Groenink M, Bouma BJ, van Dijk AP, Helbing WA et al (2008) Evaluating the systemic right ventricle by CMR: the importance of consistent and reproducible delineation of the cavity. J Cardiovasc Magn Reson 10:40
Yang HS (2017) Three-dimensional echocardiography in adult congenital heart disease. Korean J Intern Med 32(4):577–588
Yoshin aga K, Katoh C, Noriyasu K, Iwado Y, Furuyama H, Ito Y et al (2003) Reduction of coronary flow reserve in areas with and without ischemia on stress perfusion imaging in patients with coronary artery disease: a study using oxygen 15-labeled water PET. J Nucl Cardiol 10(3):275–283